

# Supplementary Material for “LoFormer: Local Frequency Transformer for Image Deblurring”

Anonymous Authors

## 1 DETAILED ILLUSTRATION ON THE HORIZONTAL AXIS OF FIG. 8 IN THE MAIN PAPER

In Fig. 8 of the main paper, we show Spa-GC-LF/HF and Freq-LC-LF/HF. Here we illustrate how to compute the frequency ratio on the horizontal axis.

As the purple boxes shown in Fig. 1, the frequency ratio for LF/HF is determined by the diagonal length of LF/HF box *w.r.t.* the diagonal length of the feature map. See  $\text{ratio}_{\text{LF}} = \frac{t_L}{T}$ ,  $\text{ratio}_{\text{HF}} = \frac{t_H}{T}$  in the top figure of Fig. 1.

For Spa-GC, we take 75% LF as an example in Fig. 1 (a), the channel-wise attention map is simply calculated on features inside 75% LF purple box. The cosine similarity of Spa-GC in the right figure in Fig. 8 in the main paper is calculated between the source attention map with different ratios of LF/HF and the target attention map with all the information.

For our Freq-LC, when including whole frequency information, we can get attention maps  $\tilde{\mathbf{A}} \in \mathbb{R}^{m \times C \times C}$ . When executing Freq-LC by a percentage ( $p \in (0, 1]$ ) of LF/HF, we get partial attention maps  $\tilde{\mathbf{A}}^* \in \mathbb{R}^{p^2 \times m \times C \times C}$ . To complete attention maps with size  $m \times C \times C$ , replicate padding is adopted to pad the rest attention maps. We take 50% LF as an example for Freq-LC-LF in Fig. 1 (b).

## 2 IMAGES WITH DIFFERENT LOW-FREQUENCY RATIOS

We provide the images with various ratios of LF in Fig. 2. As is indicated in Fig. 2, almost all the energy lies in LF, which dominates the calculation of Spa-GC.

## 3 VISUAL RESULTS

The visual results on GoPro [3], HIDE [6], RealBlur-R [5], RealBlur-J [5] and REDS [4] are shown in Fig. 3- 10. Our model yields more visually pleasant outputs than other methods on both synthetic / real-world motion deblurring. Compared with NAFNet64 [1], which has a competitive performance on GoPro dataset, Fig. 6 shows that LoFormer is much more robust than NAFNet64.

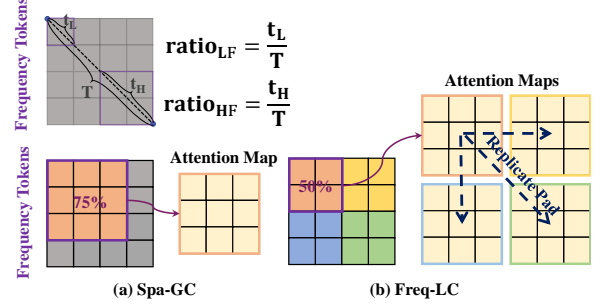


**Figure 1: Detailed illustration for Fig. 8 in the main body of the paper. For the feature in the frequency domain, we take the diagonal line as the axis of proportional selection. For the frequency feature  $X \in \mathbb{R}^{H \times W}$ , the points on the diagonal line is used to define the range of low / high frequency (LF/HF). Take the point  $X_{h,w}$  located in  $[h, w]$  as an example, the attention map with LF/HF ratio ( $\text{ratio}_{\text{LF}} / \text{ratio}_{\text{HF}}$ ) is done in the set of  $X_{i,j}$ , where  $i < h$  and  $j < w$  (LF),  $i \geq h$  and  $j \geq w$  (HF).  $\text{ratio}_{\text{LF}} = \frac{t_L}{T}$ ,  $\text{ratio}_{\text{HF}} = \frac{t_H}{T}$ , where  $t_L = \sqrt{h^2 + w^2}$ ,  $t_H = \sqrt{(H-h)^2 + (W-w)^2}$ ,  $T = \sqrt{H^2 + W^2}$ . For Freq-LC, we draw local windows with the window size  $b = 2$  for simplicity.**



**Figure 2: Images with different low-frequency ratios. Almost all the energy lies in the low frequency which represents the structure of the image.**

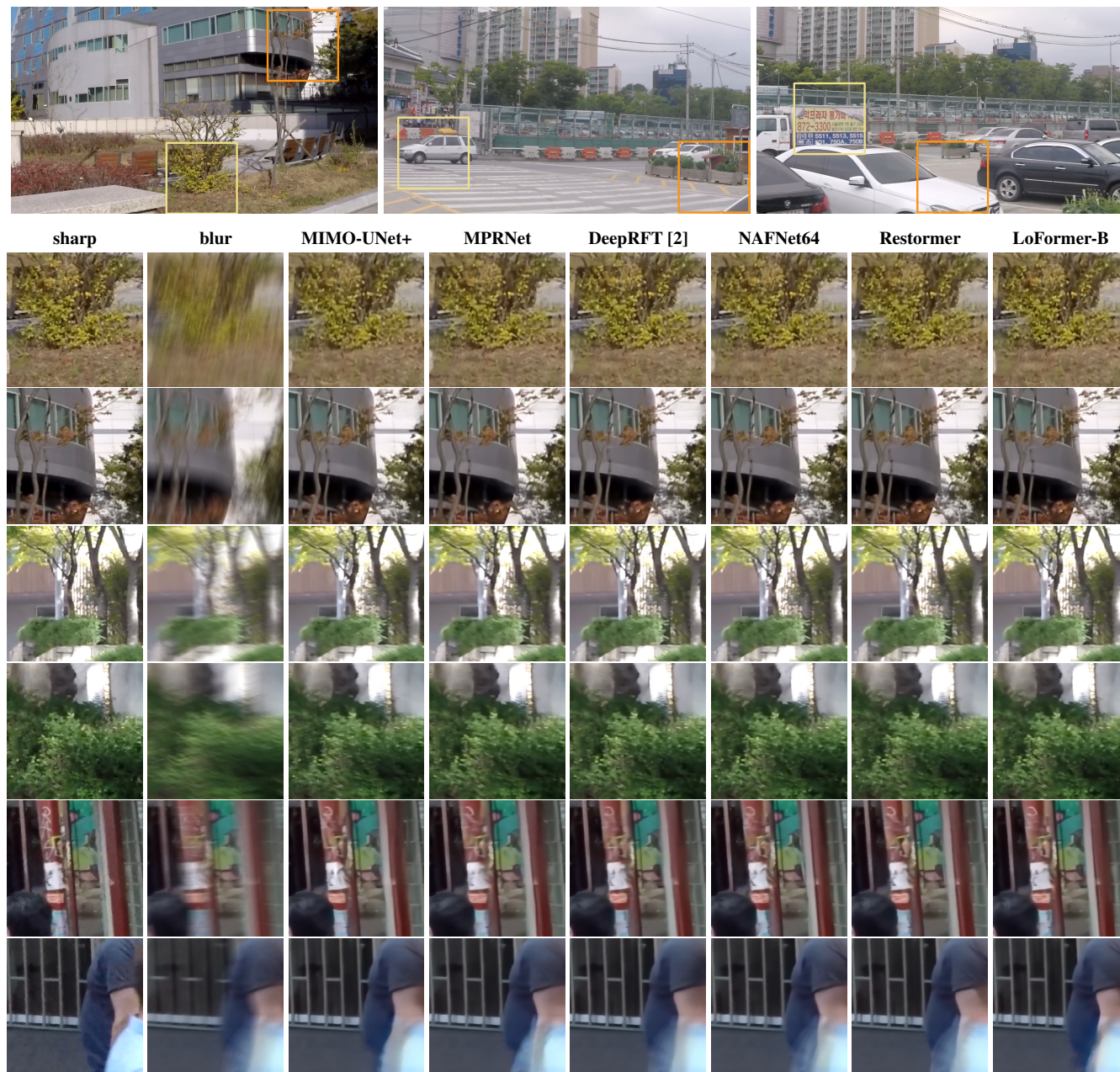


Figure 3: Examples on the GoPro test set.



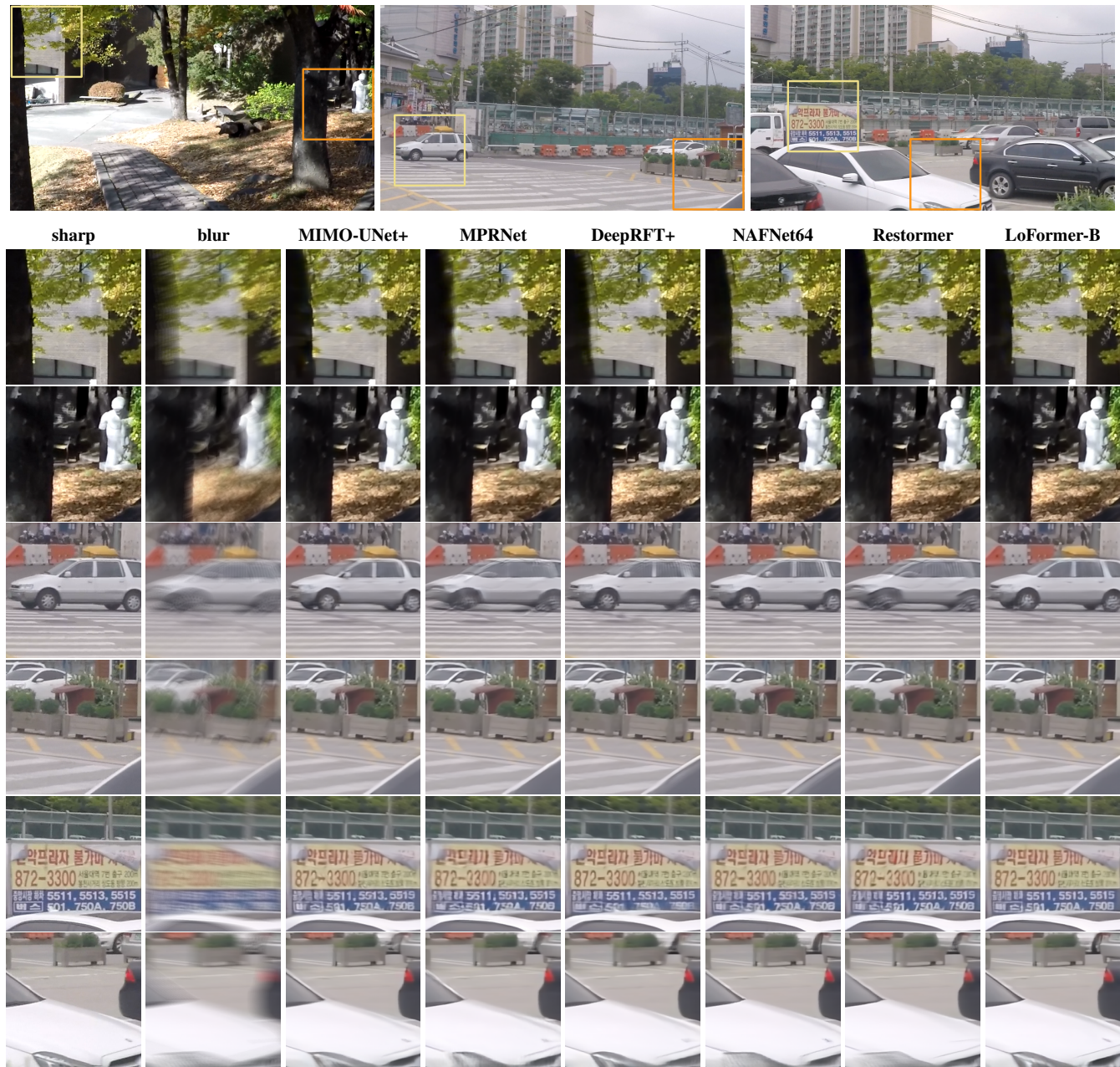


Figure 4: Examples on the GoPro test set.



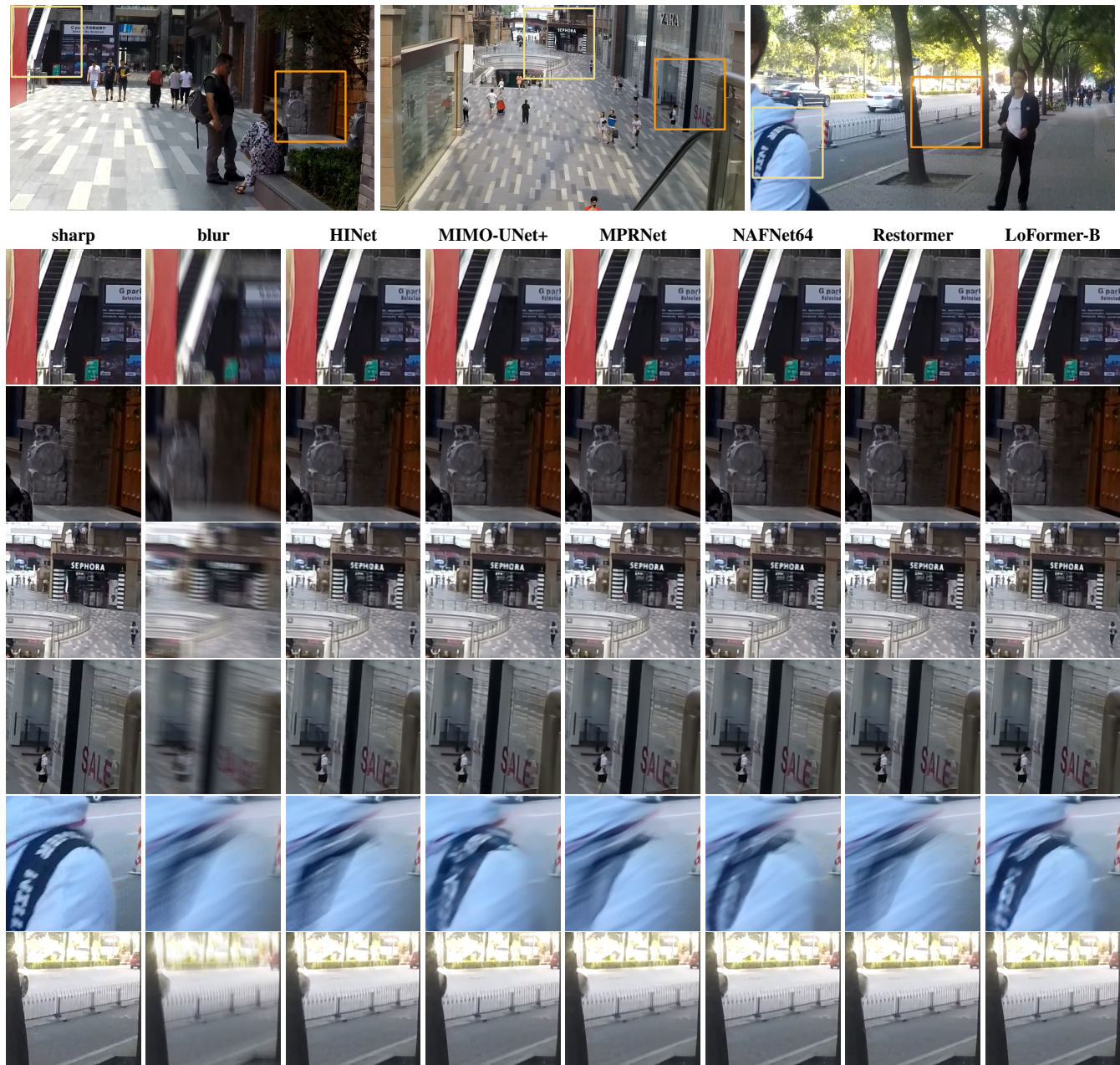


Figure 5: Examples on the HIDE test set.



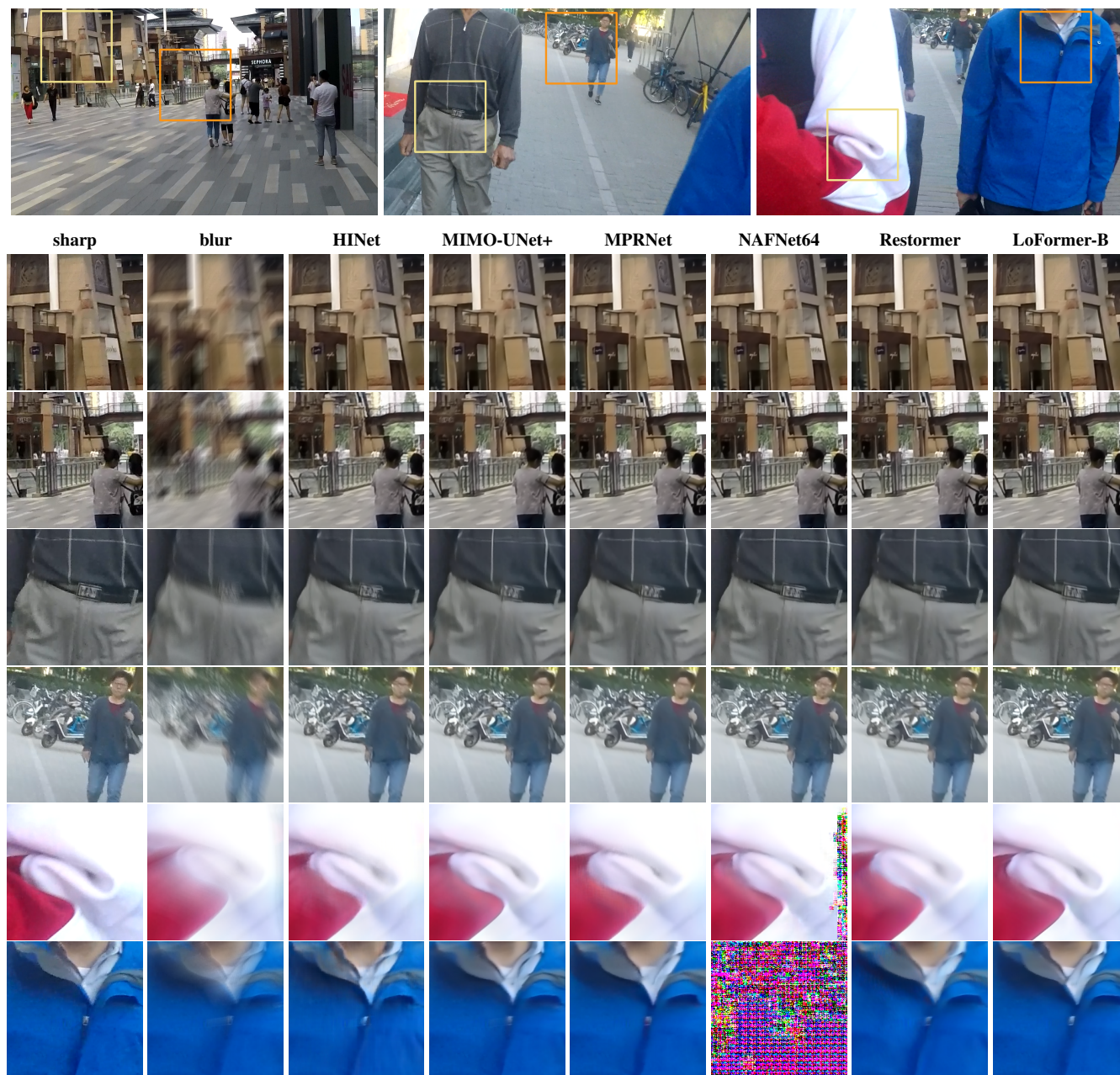


Figure 6: Examples on the HIDE test set.



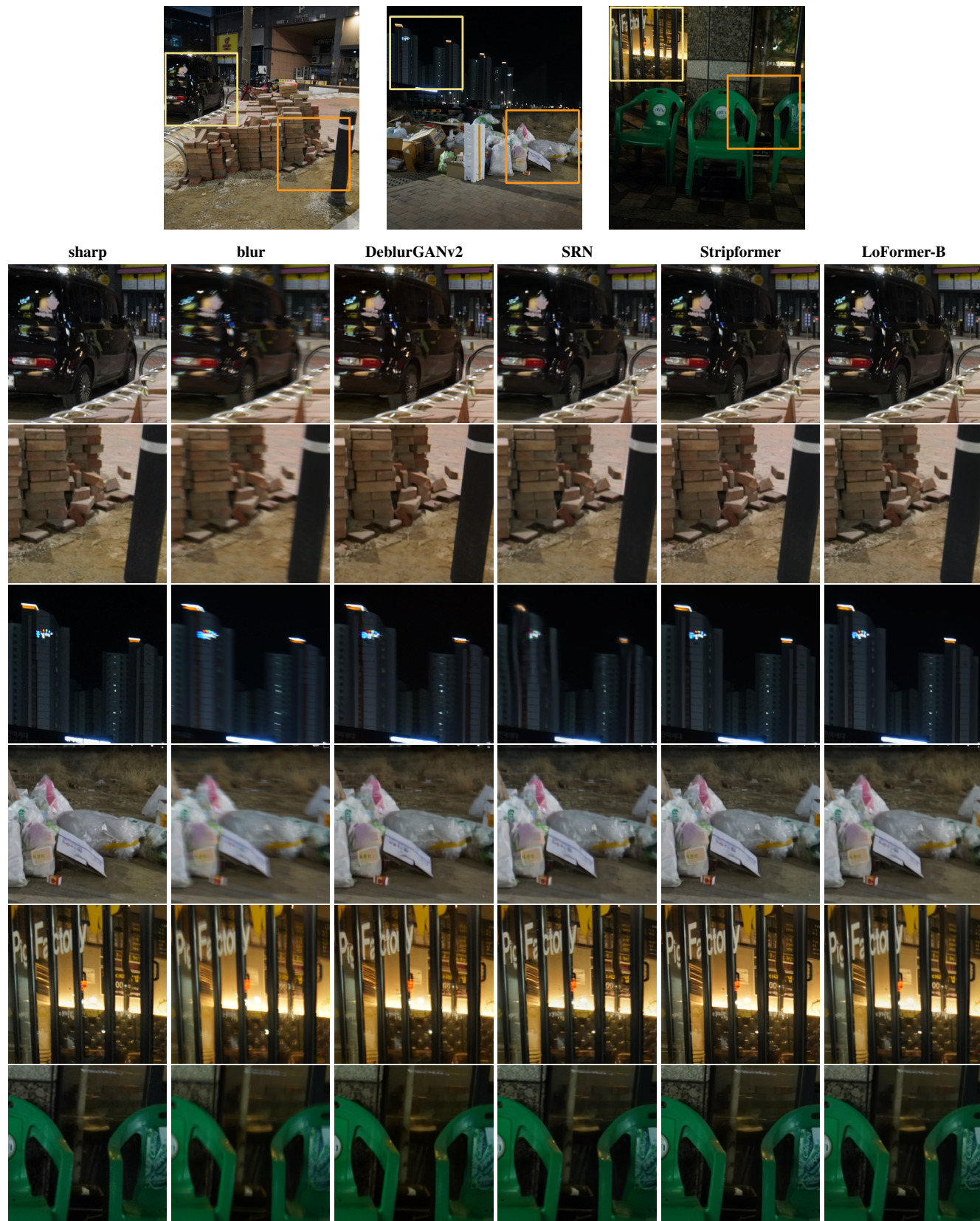


Figure 7: Examples on the RealBlur-J test set.



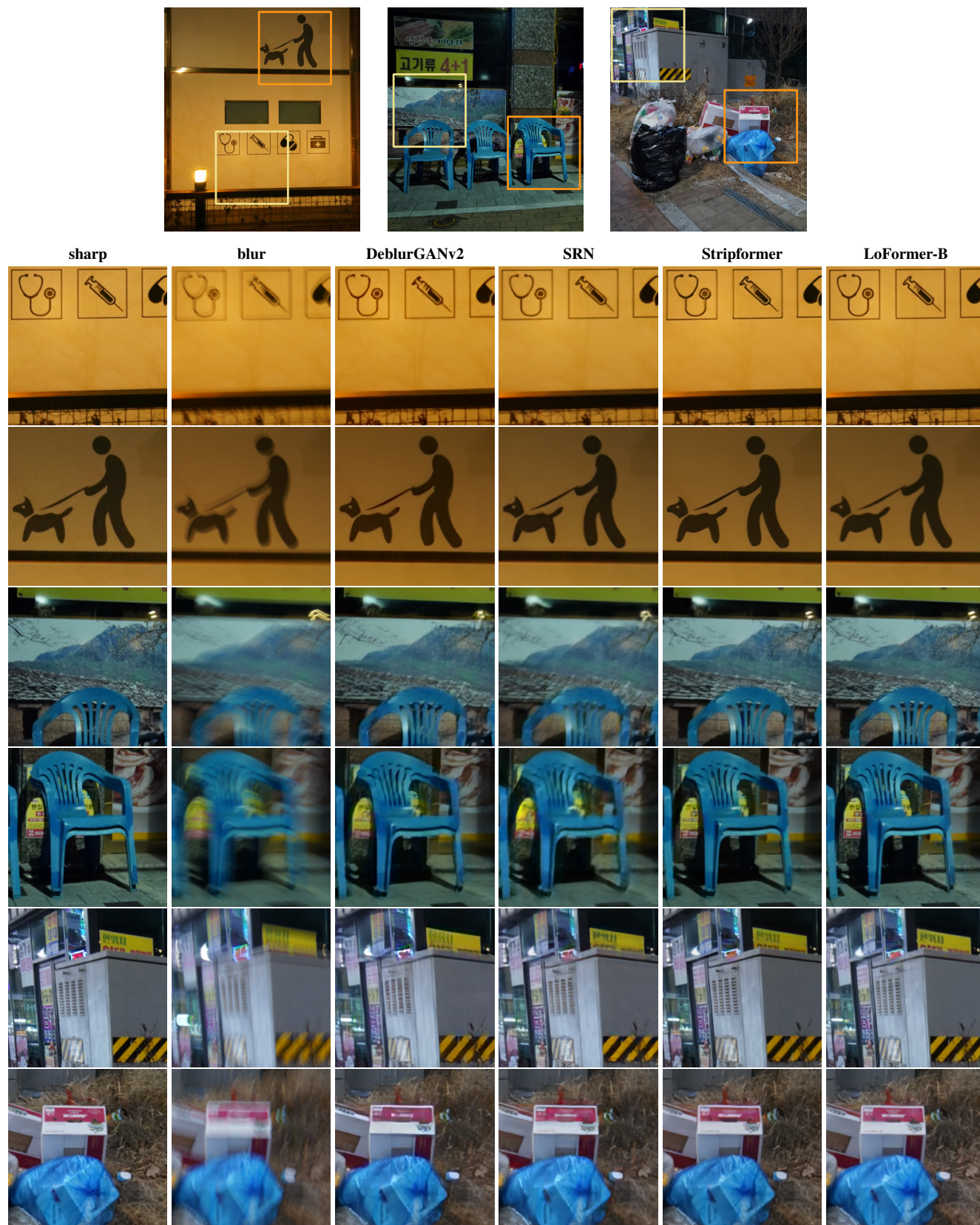


Figure 8: Examples on the RealBlur-J test set.



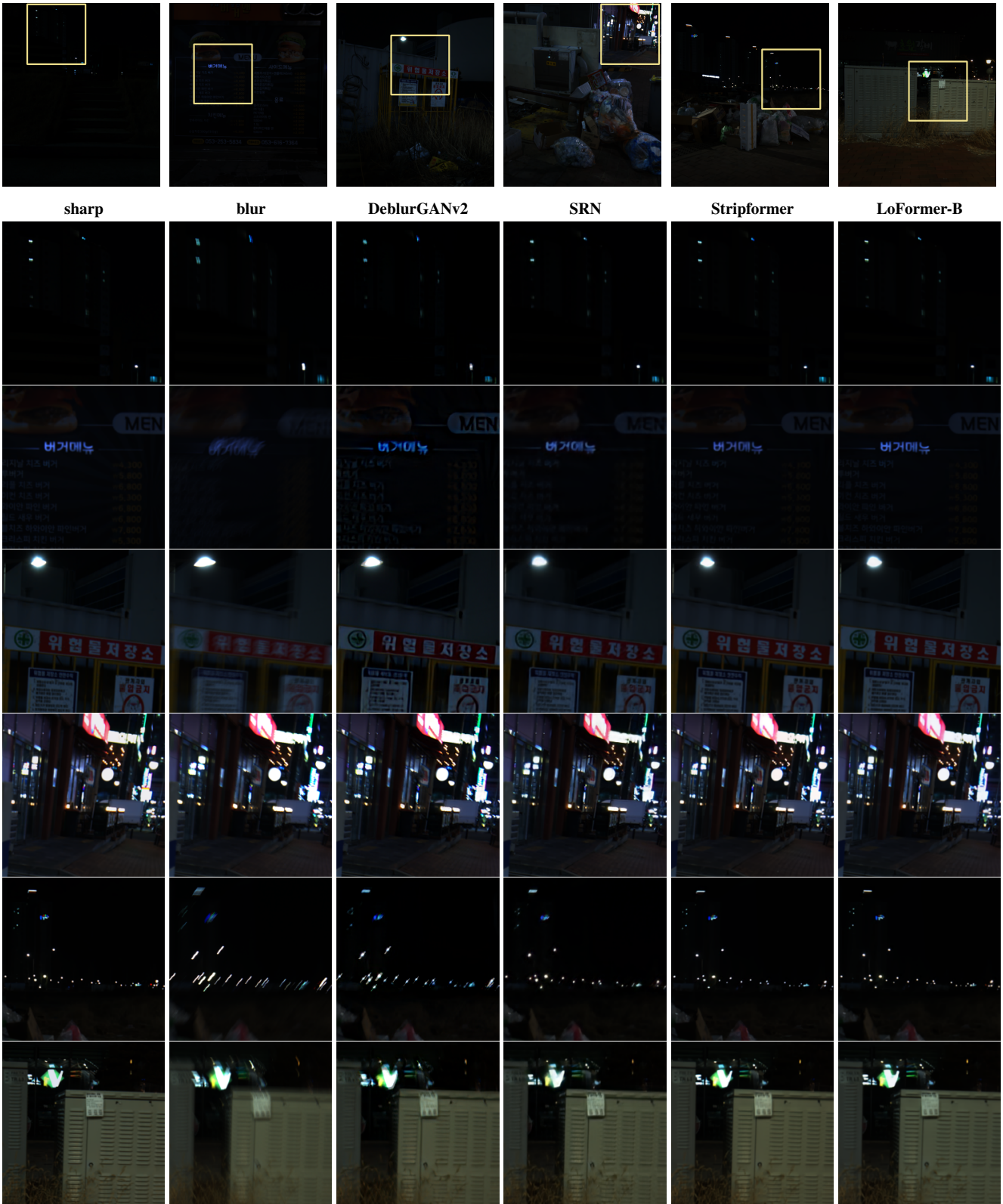


Figure 9: Examples on the RealBlur-R test set.



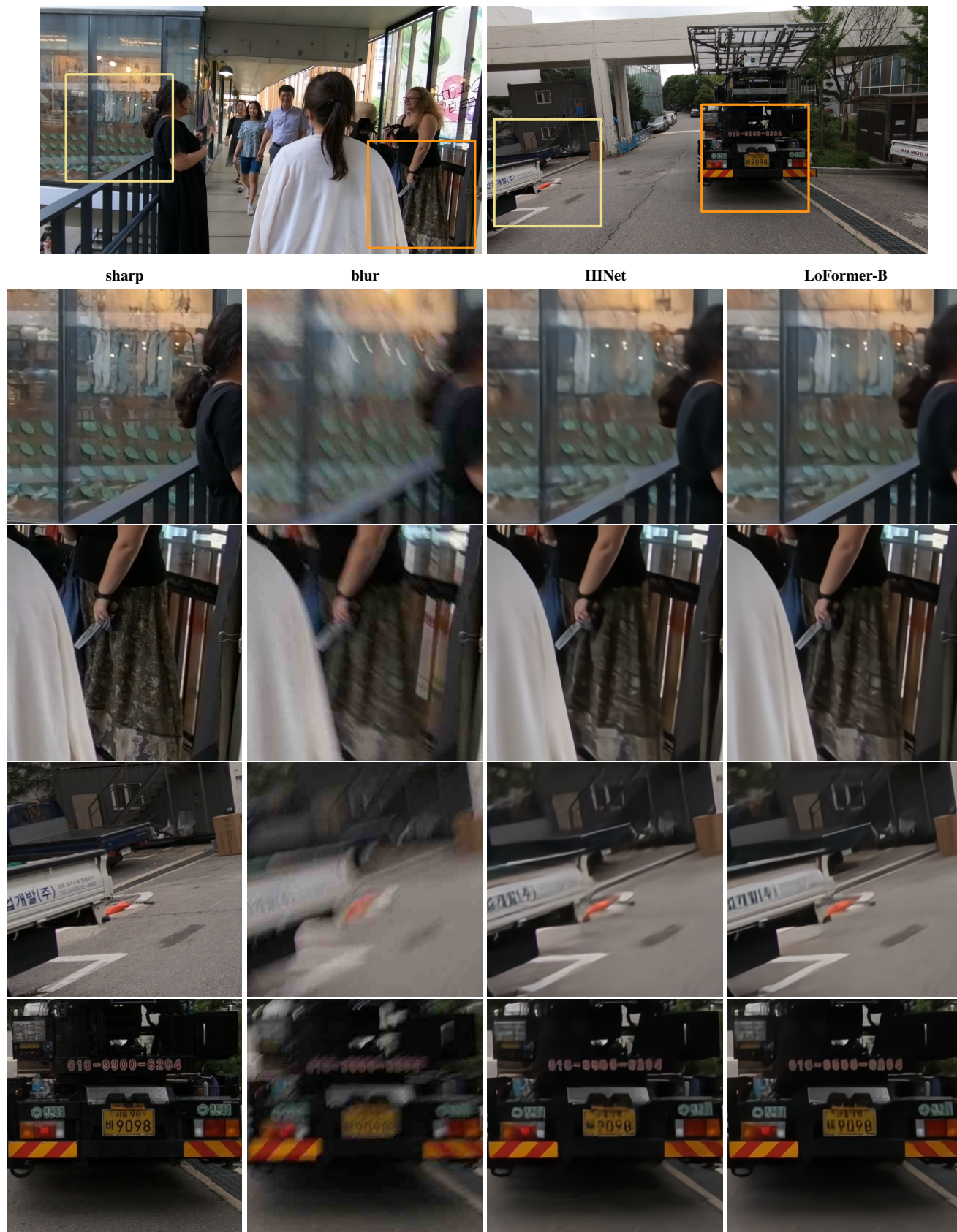


Figure 10: Examples on the REDS-val-300 set.

REFERENCES

[1] Liangyu Chen, Xiaojie Chu, Xiangyu Zhang, and Jian Sun. 2022. Simple Baselines for Image Restoration. In *Proc. ECCV*.  
[2] Xintian Mao, Yiming Liu, Fengze Liu, Qingli Li, Wei Shen, and Yan Wang. 2023. Intriguing Findings of Frequency Selection for Image Deblurring. In *Proc. AAAI*.  
[3] Seungjun Nah, Tae Hyun Kim, and Kyoung Mu Lee. 2017. Deep Multi-scale Convolutional Neural Network for Dynamic Scene Deblurring. In *Proc. CVPR*.  
[4] Seungjun Nah, Sanghyun Son, Suyoung Lee, Radu Timofte, and Kyoung Mu Lee. 2021. NTIRE 2021 Challenge on Image Deblurring. In *Proc. CVPR Workshop*.  
[5] Jaesung Rim, Haeyun Lee, Jucheol Won, and Sunghyun Cho. 2020. Real-World Blur Dataset for Learning and Benchmarking Deblurring Algorithms. In *Proc. ECCV*.  
[6] Ziyi Shen, Wenguan Wang, Xiankai Lu, Jianbing Shen, Haibin Ling, Tingfa Xu, and Ling Shao. 2019. Human-Aware Motion Deblurring. In *Proc. ICCV*.